29th International Cosmic Ray Conference Pune (2005) 3, 433-436

Design and Tests of the Scintillating Fiber Hodoscopes in the CREAM Instrument

Y.S. Yoon[a], H.S. Ahn[b], M.G. Bagliesi[c], G. Bigongiari[c], O. Ganel[b], J.H. Han[d], G. He[b], H.J. Hyun[d], J.A. Jeon[d], T.G. Kang[b], H.J. Kim[e], K.C. Kim[b], J.K. Lee[d], M.H. Lee[b], L. Lutz[b], P. Maestro[c], A. Malinine[b], P.S. Marrocchesi[c], S.W. Nam[d], N.H. Park[d], H. Park[e], I.H. Park[d], E.S. Seo[a,b], R. Sina[b], S. Syed[b], J. Wu[b], J. Yang[d], R. Zei[c], H.Q. Zhang[b] and S.Y. Zinn[b]

(a) Dept. of Physics, University of Maryland, College Park, MD 20742 USA
(b) Inst. for Phys. Sci. and Tech., University of Maryland, College Park, MD 20742 USA
(c) Dept. of Physics, University of Siena and INFN, Via Roma 56, 53100 Siena, Italy
(d) Dept. of Physics, Ewha Womans University, Seoul, 120-750, Republic of Korea
(e) Dept. of Physics, Kyungpook National University, Taegu, 702-701, Republic of Korea
Presenter: Young Soo Yoon (ysy@umd.edu), usa-yoon-Y-abs2-og15-poster

The Cosmic Ray Energetics And Mass (CREAM) instrument includes 6 orthogonal layers of scintillating fibers in three hodoscopes (S0, S1 and S2) for supplementary charge identification and particle tracking information. An additional single layer detector (S3) is included for triggering purposes. Hodoscopes S0 and S1 are located directly above the upper of two carbon interaction targets, and S2 is positioned between the two targets. S3 is located between the lower target and the calorimeter. Since each fiber has slightly different properties, light yields and attenuation curves of fibers in S0, S1, and S3 were studied individually. These fiber characteristics and results of beam tests performed at CERN in Nov 2003 are presented. Simulation results for energy deposits in S3 are also discussed.

1. Introduction

The CREAM payload is designed to fly at the top of the atmosphere, suspended under a NASA balloon, to directly measure cosmic-ray nuclei from H to Fe, in the energy range from ~10^{12} to ~10^{15} eV. The CREAM instrument, described in more detail elsewhere in this conference [1] is comprised of several complementary detector systems to measure directly the charge and energy of cosmic rays, including a 20 radiation length (X_0) sampling tungsten/scintillating-fiber calorimeter preceded by a pair of graphite targets, each ~0.25 λ_{int} or 9.5 cm in depth. Above the targets is a silicon charge detector (SCD) [2] comprised of over 2900 pixels, each ~2.1 cm^2 in area, intended to measure the charge of incident cosmic-ray nuclei with a resolution of ~0.2e. For high energy showers, a significant number of secondary shower particles are thrown back in the upwards direction, generating signals in the SCD, mostly near the point through which the incident nucleus traversed the SCD. Such back-scatter can and does make it more difficult to correctly identify the charge of the incident nucleus. To minimize this disturbance, the shower axis must be reconstructed from the signal pattern in the calorimeter. Adding more measurement points above the calorimeter, using scintillating fiber hodoscopes (S0/S1 and S2) interleaved with the target layers, improves the tracking accuracy and thus the accuracy of charge identification. See reference [3] for the tracking algorithm and the position resolution based on Monte Carlo simulations. In addition to the detector systems mentioned above, CREAM includes a Transition Radiation Detector (TRD), and a Timing-based Charge Detector (TCD) [4], above the SCD. The TCD provides charge measurements for those particles traversing the TRD. To do so, the TCD requires a time reference point in those cases where a significant number of particles are scattered back from the calorimeter. This is provided by the S3 single-layer scintillating fiber detector, which is read out from both sides using high-speed photo multiplier tubes (PMTs). The S3 signal is also used in the TCD trigger to provide an indication that a charged particle that has traversed the TCD has also generated a calorimeter shower. The hodoscope readout system is designed around HPDs as these devices combine low power (~0.8

W including front end electronics and high voltage), low weight (~30 grams per unit), high channel count (up to 73 channels per unit), compact size (~30 cm^3 per unit), and very uniform gain between pixels (~5% RMS) and between HPDs (~10% RMS at the same HV setting).

Figure 1. Photograph of hodoscope clear fibers and aluminum cookies.

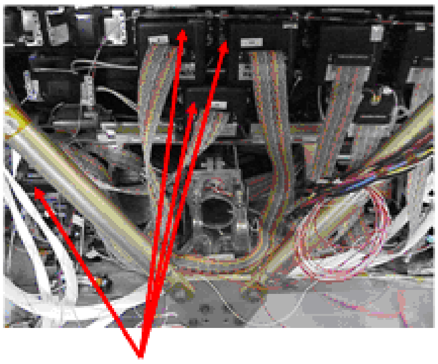

Figure 2. A set of two S0/S1 HPD boxes (top), one S2 HPD box (bottom), and a Motherboard box (left)

2. Design and tests

The S0/S1 hodoscope is located at the top of the upper target, and is comprised of four layers of Bicron BCF-12MC multi-clad scintillating fibers. Each fiber is square with a 2x2 mm^2 cross-section, with a thin layer of white extra-mural absorber (EMA) painted over the external cladding layer. Each fiber is cut and polished on both ends, with vacuum-deposition of aluminum on one end forming a mirror to increase the effective light yield and reduce the dependence of signal strength on position of particle traverse through the fiber. For mechanical reasons alternate fibers are read out from opposite ends. Alternate layers have orthogonal fiber orientation relative to each other, with 2 layers reading in the X orientation, and 2 others in the Y orientation. Each layer has a total of 360 fibers covering an area of approximately 770×770 mm^2. Each fiber is glued on the readout side to a short segment of clear fiber also painted with white EMA. The clear fibers are bent and routed into aluminum cookies that align the clear fibers with pixels of the HPD as shown in Fig. 1. Each HPD reads out 30 fibers from S0 (upper pair of layers) and 30 more from S1 (lower pair of layers). The S0/S1 detector readout thus includes 24 HPDs. The S2 hodoscope[5] has a similar structure, but with an active area of only 630×630 mm^2, as it is located between the flared targets and thus has a smaller aperture to cover. S2 is also comprised of only 2 layers, and thus requires only 12 HPDs to be fully read out. All 36 HPDs are powered in sets of 3 (2 S0/S1 HPDs and 1 S2 HPD), with the high voltage supply connected to the HPDs via special HV cables (see Fig. 2).

During the design phase of the hodoscopes, various other options were considered. Figure 3 shows the response of 1×1 mm^2 fibers vs. 2×2 mm^2 fibers to β particles from a collimated ^{106}Ru source, as a function of distance from the PMT used for test readout. The readout was triggered by a second PMT, reading out a 1cmx1mm piece of 1cm thick scintillator, which assured that the incident β particle fully traversed the fiber being tested. The noise from the readout electronics was estimated as equivalent to ~3.3 photo-electrons at an HPD gain of 2000. Requiring a minimal S/N of 3, the figure shows that beyond 35 cm from the HPD, the 1×1 mm^2 fibers would provide an insufficient light signal. In addition, using the thicker fibers reduced the channel count by half, reducing both the power requirement, and the complexity of the readout electronics. The higher light yield afforded by the thicker fibers, as well as the reduced number of channels needed with these, led to the choice of the 2×2 mm^2 fibers. Figure 4 shows a similar test comparing fibers with no EMA, fibers with white EMA and fibers with black EMA, each with and without aluminized mirror on the non-readout end, with each fiber ~50 cm in length, and measurements made at 5 cm intervals starting from about 10 cm away from the PMT to about 45 cm away. While the non-EMA fiber with mirror had a much greater light yield than any other type, the non-uniform response over the length of the fiber dictated the choice of white EMA fibers with mirroring. These had about 60% of the non-EMA mirrored fiber response near the readout end, but nearly 80% of the non-EMA mirrored fiber response near the mirrored end. The change in signal over the length of the fibers improved from ~35% drop to only 16% drop with respect to the highest signal. The reason for these results is that non-EMA fibers have a significant contribution from so-called "cladding light", i.e. light which does not remain within the fiber core, but is rather reflected only at the interface between the cladding and air. The attenuation length for cladding light is much shorter than that of the core light, so it is seen mostly from short fiber distances. Cladding light travels about ¼ of a wave length outside the cladding every time it is reflected through total internal reflection. When EMA is present, and especially when this EMA is black, a large fraction of the cladding light is absorbed in the EMA and the attenuation length for the cladding light is drastically shortened, to the point that even a few cm away from the PMT it does not contribute to the collected signal in any significant way. Figure 4 also shows that mirroring the fibers increases the effective light yield by about 60%, and reduces the signal drop from one end of the fiber to the other by nearly half. The same effects seen in Figure 4 can also be seen clearly in Figure 5, which displays the results for 75 cm long fibers (similar to the S0/S1 fiber length). The comparison of a white EMA mirrored fiber of 50 cm length to one of 75 cm length shows a typical fiber to fiber variation of ~10%.

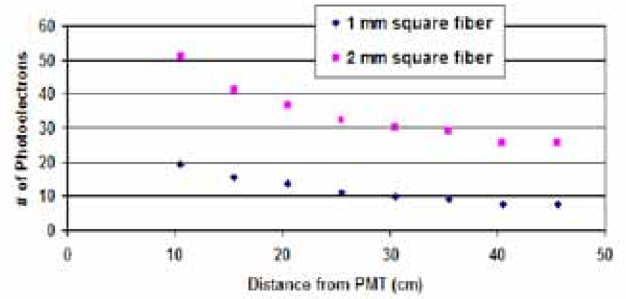

Figure 3. Light yield comparison for fibers with different thicknesses using a collimated ^{106}Ru source.

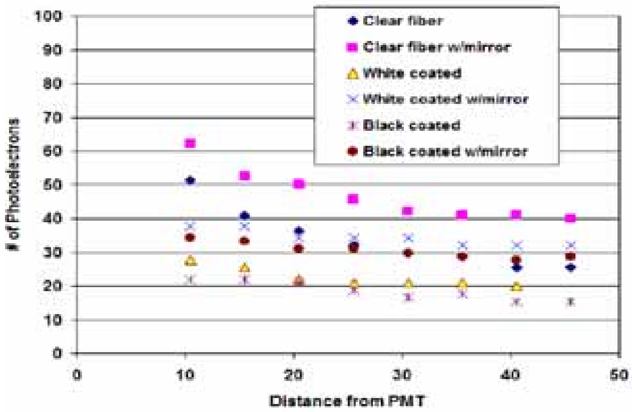

Figure 4. Light yield comparison of various fiber types with 50 cm length using a collimated ^{106}Ru source.

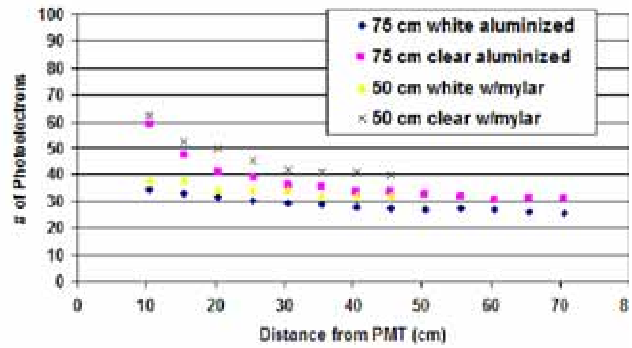

Figure 5. Light yield comparison for fibers with 75 cm length using a collimated ^{106}Ru source.

3. Beam test results of S0/S1

The hodoscopes were calibrated with fragments of the Indium beam at CERN in September 2003. Figure 6 shows a scatter plot comparison between a charge measurement using the SCD and a charge measurement using S0/S1 (based on the sum of signals in the two x-oriented layers). The SCD clearly separates the different elements. The S0/S1 hodoscope can also separate elements to some extent, and can certainly separate charge groups. The slight bend in the overall shape of the plot is most likely due to saturation effects in the scintillator for nuclei with high charges where ionization is very dense near the particle track.

4. Simulation study of S3

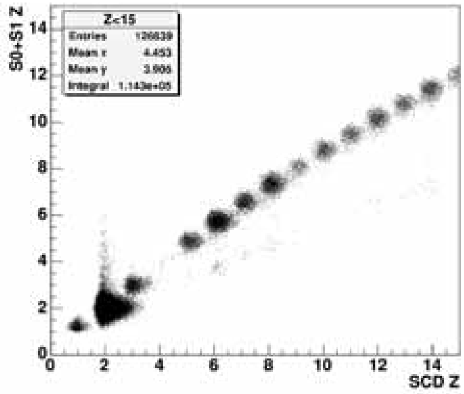

Figure 6. Beam test data show clear correlation between S0/S1 and SCD charge measurements.

The main purpose of the S3 detector, as mentioned above, is to provide a reference time and a shower flag for the TCD. Simulations of proton showers at energies of 100 GeV, 500 GeV, 1 TeV, and 10 TeV were used to produce a scatter plot between the total energy deposit in the calorimeter and that in S3. As shown in Fig. 7, there is a fairly high correlation between these two deposits, showing that the S3 detector provides a good shower flag, especially at higher energies. The greater spread in the vertical direction is due to the obviously poorer energy resolution obtainable from S3, a single layer of fibers relative to a 20 X_0 calorimeter. The horizontal line at 4 MeV is where we expect to measure 100 photoelectrons in the S3 readout. This is the minimum light yield needed to provide a good time resolution for the TCD. Most 100 GeV showers can be seen to provide a signal above this threshold. Since the amount of back-scatter is roughly logarithmically dependent on the incident particle energy, good timing accuracy is more important at higher energies than at 100 GeV. Very few showers at 1 TeV or higher fail to produce a signal of over 100 photoelectrons.

5. Conclusions

The hodoscopes in CREAM provide useful tracking information, with some charge identification provided by S0/S1. Lab measurements directed the design towards 2×2 mm^2 fibers with multiple cladding, white EMA, mirroring on the non-readout end, and clear fibers for routing the light signal to the HPDs. The S3 detector has been shown to have sufficient light yield in shower events in the energy range of interest to provide both a reference time of sufficient resolution for the TCD to reject back-scattered particle signals, and to provide a fast shower flag for the TCD trigger without resorting to the calorimeter system.

6. Acknowledgements

This work was supported by NASA. The authors thank CERN for its excellent beam test facilities and operations.

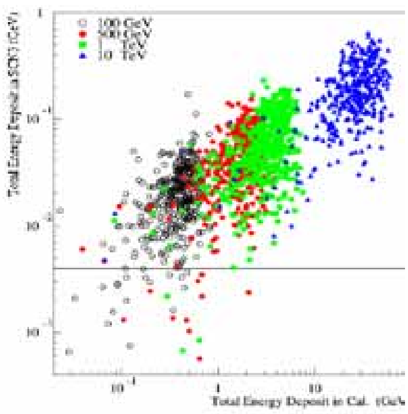

Figure 7. Correlation between S3 and calorimeter energy deposits.

References

[1] E. S. Seo et al., Proc. 29th ICRC, Pune, OG1.1 (2005).
[2] I. H. Park et al., Proc. 29th ICRC, Pune, OG1.5 (2005).
[3] H. S. Ahn et al. Proc. 27th ICRC, Hamburg, 6, 2159 (2001).
[4] S. Coutu et al., Proc. 29th ICRC, Pune, OG1.5 (2005).
[5] P.S. Marrocchesi et al. ,
Nucl. Phys. B (Proc. Suppl.) 134 (2004) 75-77